Stability Detection of Building Bearing Structure Based on Bim and Computer Vision

Lin Wu(✉) and Shunbin Wang

ZaoZhuang Vocational College of Science and Technology, Zaozhuang 277599, China
zzkjzyxy_bim@126.com

Abstract. The stability of building load-bearing structure is closely related to the building life. Unstable building load-bearing structure has a great potential safety hazard. The stability detection method of building load-bearing structure based on BIM and computer vision is designed. The computer vision system for image acquisition of building load-bearing structural components is designed, which is composed of CCD camera, image acquisition card, light source and UAV. The secondary development technology of Revit is applied to establish the overall structural information model, and the influencing factors of structural stability are introduced into the information model. Build a stability detection network model based on YOLOv4 network architecture, and implement the stability detection of building load-bearing structures. The test results show that the accuracy rate of the design method is higher than 0.920, the recall rate is higher than 97%, and the test time for new and old buildings is 106.85 min and 75.41 min respectively under different confidence levels.

Keywords: BIM · Computer Vision · Structural Information Model · Building Load-Bearing Structure · Stability Test

1 Introduction

During the long-term use of engineering structures, under the action of internal or external, artificial or natural factors, material aging and structural damage will occur as time goes by, which is an irreversible objective law. Such damage accumulation will lead to deterioration of structural performance, reduction of bearing capacity and durability. If the law and degree of such damage can be scientifically evaluated and effective treatment measures can be taken in time, the process of structural damage can be delayed and the purpose of extending the service life of the structure can be achieved [1]. Therefore, the reliability evaluation method and reinforcement technology of existing structures have become a hot issue in the engineering field. Many engineering technicians and research groups have turned their attention to this field, and put the identification and reinforcement technology of engineering structures in a very prominent position. Among them, the stability detection of building load-bearing structures is an important research content.

B. Wang et al. (Eds.): ICMTEL 2023, LNICST 533, pp. 137–150, 2024.
https://doi.org/10.1007/978-3-031-50574-4_10

Structural reliability refers to the ability of the structure to complete the predetermined functions within the specified time and under the specified conditions. The specified time refers to the design service life of the structure, and the specified conditions refer to the normal design, normal construction, normal use and maintenance. The intended functions include safety, applicability and durability [2]. The purpose of engineering structure design is to use the performance of the structure to complete the predetermined function of the design. Its main function is to transmit and resist various actions of human or nature through the structure, so that the building can complete the predetermined function within the specified time and under the specified conditions.

Reference [3] proposes a building stability detection method based on edge feature fusion. This method uses an encoder network to fuse the RGB feature map and edge feature map of the building, and calculates the weight of the fused feature map. Through the weighted processing of the weights, the stability detection is completed. Reference [4] proposes a building stability detection method based on convolutional neural network. This method improves the feature extraction network in the Mask-RCNN model and designs a multi-scale group convolutional neural network with an attention mechanism. The convolutional neural network is used for feature training to complete stability detection.

Although the above methods can complete the stability detection, the acquisition accuracy of building data is low, resulting in poor stability detection performance. Therefore, a building load-bearing structure stability detection method based on BIM and computer vision is proposed. This method first uses computer vision technology to collect the images of building load-bearing structure components, then builds the BIM model of building load-bearing structure, and finally uses YOLOv4 network architecture to complete the detection of building load-bearing structure stability.

2 Stability Testing of Building Load-Bearing Structures

2.1 Image Collection of Building Load-Bearing Structural Components Based on Computer Vision

The image of building load-bearing structure is collected based on computer vision technology. A computer vision system for image acquisition of building load-bearing structural components is designed, which consists of a CCD camera, an image acquisition card, a light source, and an unmanned aerial vehicle.

First design a complete CCD camera that integrates image acquisition, transmission and display. The CCD image sensor selects KAI-01050 image sensor, whose resolution and frame rate meet the design requirements of the camera, and the size of a single pixel and the overall The image sizes are all larger, so the image quality is higher and the image is sharper.

The normal operation of CCD sensor requires external complex line and field signals to drive, and the collected image is an analog signal. The digital image can be obtained only after the A/D conversion through the relevant double sampling chip. If discrete devices are used to realize the functions of driving and analog-to-digital conversion, the image acquisition circuit will be very complex, which not only increases the difficulty of software and hardware debugging, but also is difficult to meet the size requirements of

the image acquisition circuit board. Therefore, the camera selects AD9920A chip from Analog Devices as the analog front-end image acquisition chip, and its main parameters are shown in Table 1.

Table 1. AD9920A chip main parameters

Serial No	project	parameter
1	Data bit width/bits	Fifteen
2	Sampling frequency/MSPS	Fifty-two point five
3	Is the horizontal signal programmable	Yes
4	Is the vertical signal programmable	Yes

The sampling rate of AD9920A chip can reach the data rate of KAI-01050 image sensor selected in this subject. Therefore, AD9920A chip is selected to generate various driving signals required by CCD.

The sensor chip used in this project has a resolution of 1024X 1024 under four channels, a frame rate of 120fps, and a data rate close to 1Gibps. The USB3.0 interface can reach the actual transmission rate of 3.2Gbps, which can meet the design requirements, and at the same time supports hot swapping, which is easy to use, and all mainstream PCs have this interface. Therefore, this topic chooses USB3.0 as the data transmission channel.

The overall structure of the designed CCD camera is shown in Fig. 1.

The image acquisition module configures the register inside the AD9920A chip through the C8051F921 single-chip microcomputer to generate the horizontal and vertical driving signals that drive the CCD to work normally. The horizontal signal needs level conversion to drive the KAI-01050 CCD sensor to collect images. The collected analog image data is sent back to the AD9920A for correlation double sampling, and the 12 bit digital image data obtained is transmitted to the main controller FPGA of the data transmission module with the same line (HD), field (VD), and data (DCLK) synchronization signals. At the same time, the C8051F921 microcontroller in this module is also responsible for receiving various parameters sent by the upper computer, such as the amplification gain of analog signals, exposure time, number of row blanking pixels, sampling points of correlated double sampling, etc. After receiving the parameters, the microcontroller configures the register of AD9920A to change the working state of CCD according to the parameters.

The main controller of the data transmission module selects the cyclone II FPGA of Altera Corporation, and the USB3.0 transmission selects the CYUSB3014 chip of Cypress Corporation. After receiving the digital image from the image acquisition module, the FPGA first performs data buffering and data bit width transformation through FIFO (FirstInFirstOut), and then sends the data to the CYUSB3014 chip according to the USB3.0 timing requirements. After the chip receives the data, it uploads the data to the host computer through the batch transmission mode according to the USB3.0 protocol [5, 6].

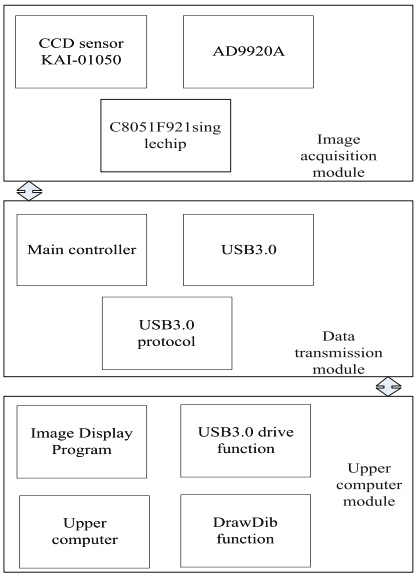

Fig. 1. General structure of the designed CCD camera

The image display program of the upper computer module uses MFC and multithread programming, receives image data with the USB3.0 driver function provided by Cypress, writes the data to the two image buffers of the upper computer through ping-pong operation, and displays the image data through DrawDib function. The image display interface of the upper computer can set parameters to control the camera working in different states.

System workflow: After the system is powered on, the single-chip microcomputer configures the internal registers of AD9920A through the SPI bus to generate the horizontal, vertical and exposure signals that drive the CCD to work. The analog image collected by the CCD is converted into a digital signal by AD9920A correlated double sampling, and sent to the FPGA of the data transmission system. The FPGA buffers the image data through the FIFO, converts the 8bit image data into 32bit, and then sends the data to the USB3.0 chip through the state machine.After receiving the data, the USB3.0 chip forwards the data to the USB3.0 interface through its internal DMA channel, and sends the data to the upper computer through batch transmission. The upper computer uses the driver interface function provided by Cypress to receive data and display images through the application program.

The design of the image acquisition card is shown in Fig. 2.

The designed acquisition card is mainly composed of image acquisition interface, core controller, external memory and data transmission bus interface.

At present, the CameraLink protocol has gradually become a general image transmission protocol, and the CameraLink interface standard is based on the standard interface defined by the Camera Link protocol, and the interface uses LVDS to transmit signals,

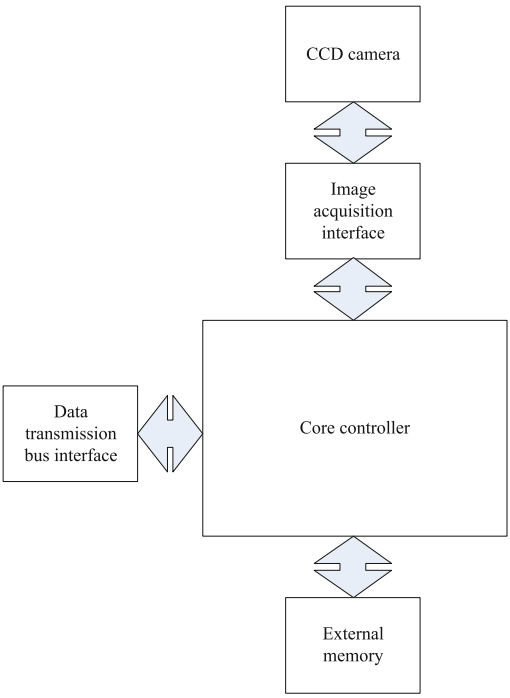

Fig. 2. Design of frame grabber

which has great advantages in transmission rate, so Camera Link is used. The interface acts as an image acquisition interface.

The image acquisition card has high requirements for real-time performance. When image acquisition is carried out, the image frame synchronization and line synchronization signals must be accurately captured to obtain complete and effective images. And in order to ensure the continuity of the image, image data buffer and corresponding logic control are also required to transmit to the PC accurately. In addition, the controller also needs to set parameters and trigger the camera. This series of actions requires strict requirements on timing. Therefore, FPGA is used as the core controller.

Because the image data transmission rate is very fast and the amount of data is large, and the internal resources of the FPGA are limited, it is not enough to cache large batches of image data, so the current relatively advanced and mature DDRII SDRAM is used as the external memory for caching, and the FPGA controls the data.

In order to meet the requirements of real-time image processing and high resolution image, the image acquisition card must have a high bus transmission rate. As a new generation of I/O serial bus standard, PCIe bus has an effective data transmission bandwidth of 250 MB/s for x1 channel and 1 GB/s for x4 channel, which is much higher than PCI bus. Therefore, the x4 channel PCIe bus interface is selected as the bus transmission interface of the image acquisition card, which can meet the requirements of high image resolution and real-time image processing.

First, the PC correctly configures PCIe through the underlying driver to make the PCIe interface work normally. Then the PC sends camera related setting instructions to the FPGA through the PCIe bus, and the FPGA sends the instructions to the camera in the form of serial port data by using the prepared serial port program. The camera receives the instructions to set and output images. The acquisition card receives the image data through the Camera Link interface, extracts the effective image according to the line field synchronization signal, and then caches the image to DDR2.At the same time, the number of image lines is counted inside the FPGA to determine the completion of a frame of image transmission. If a frame of image transmission is completed, the PC is notified to initiate a command to receive image data, and the FPGA reads the data from DDR2 and sends it to the PC through the PCIe bus. Machine. Since the PCIe bus transmits data faster than the capture card can receive images from the Camera Link interface, and DDR2 can read and write at the same time, while the data is sent to the PC, the camera output image can be uninterrupted, thus ensuring the continuity of the image.

The light source is LED light source, and its preparation equipment is shown in Table 2.

Table 2. LED light source preparation equipment

Serial No	Equipment name	Specification and model
1	LED test fixture	3028
2	LED test power supply	LED260E
3	High precision spectrometer	FR-23
4	Integrating sphere	G5000
5	Dispenser	ME32
6	Special oven	DF453
7	Coater	V100
8	Electronic balance	MN342S

Preparation plan: The solid crystal and wire bonding process in the sample preparation process is completed by the enterprise sample line, so the preparation process mainly starts from the preparation of fluorescent glue. The specific process is as follows:

(1) First, add silica gel into the rubber cup. Weigh the silica gel of A and B models according to the ratio of 1:10. First add A glue, then add B glue; Secondly, the phosphor material is added according to the amount determined in advance; Finally, anti settling starch was added, and the amount of anti settling starch was 0.12% of the amount of silica gel.
(2) The prepared mixture of phosphor, silica gel and anti sedimentation starch is homogenized and vacuumed. The mixture is stirred at 1000 rpm, 800 rpm and 1000 rpm for 2 min respectively. After stirring, the mixture is vacuumed to eliminate bubbles and mix the mixture of phosphor, silica gel and anti sedimentation starch evenly.

(3) Pour the prepared fluorescent glue into the syringe of the dispensing machine, and evenly dispense a fixed amount of fluorescent glue into the LED bracket that has been solidified and welded, and the fluorescent glue and the cup of the bracket are flush or slightly concave.
(4) The LED brackets that have been dispensed are placed in an oven for baking, and the baking conditions are 90 min at 80 °C, 90 min at 120 °C, and 180 min at 150 °C.
(5) After the baking is completed, test with a testing instrument.
(6) The drone selected is the DJI Mavic 2, which is used to carry other acquisition equipment.

2.2 Build the BIM Model of the Building's Load-Bearing Structure

BIM model of building load-bearing structure based on BIM technology. Specifically, the Revit secondary development technology is used to establish the overall structural information model, and the attributes of the influencing factors are customized by editing the shared parameters to complete the function of parameter setting of the influencing factors of structural stability. And the influence factors of structural stability are imported into the information model [7].

According to the material level, component level and structure level, the information model of influencing factors of concrete structure stability is constructed.

Firstly, the information of material hierarchy is added to the information model of influencing factors of concrete structure stability. The damage caused by material properties includes freeze-thaw damage, water permeability, chloride ion corrosion, carbonization, reinforcement corrosion, sulfate corrosion, alkali aggregate reaction and concrete cracking caused by volume stability. Next, carbonation, steel corrosion, and concrete shrinkage and creep are added to the building information model.

Taking carbonation as an example, the carbonation mechanism and the reaction process of cement in the hydration process are regarded as the LOD100 level and established in the information model. LOD200 mainly stores the information of the carbonation depth prediction model, among which the cement dosage, cement type, water-cement ratio and aggregate have an important influence on the carbonation depth. LOD300 stores the evaluation index of carbonization and the influence of carbonization on structural stability in the structural stability information model.

There are many influencing factors of reinforcement corrosion, including carbonization, chloride ion erosion, thickness of protective layer, reinforcement material, reinforcement corrosion rate, environmental factors, etc. The function of rebar creation in concrete components is realized through secondary development of Revit.

Then, factors such as reinforcement corrosion rate are added to the created reinforcement properties, which is equivalent to considering the influence of reinforcement corrosion in the model. LOD100 stores relevant information from the perspective of material damage, such as the decrease of cohesive force caused by insufficient thickness of concrete protective layer. LOD200 stores relevant information data at this level from the perspective of electrochemical corrosion process of reinforcement.

The shrinkage and creep of concrete need to be detected during the whole life cycle of the building. This feature gives full play to the advantages of the building information model. It is necessary to establish a 3D model according to the design criteria of standard

components. By testing, the model analysis of the whole life cycle of the building can be realized.

Secondly, the information of component hierarchy is added to the information model of influencing factors of concrete structure stability. The theoretical research on concrete corrosion cracking is mainly conducted from the perspectives of material damage, crack extension, etc. The current research mainly focuses on the critical corrosion rate of concrete corrosion cracking, and the layered research on corrosion cracking is conducted through the reinforcement corrosion rate [8]. The research on bond performance between reinforcement corrosion and concrete mainly analyzes the change of bond strength between reinforcement and concrete, as well as the deformation caused by the stress transmission between them. The bond performance between reinforcement and concrete is evaluated through the change of bond strength, which is taken as the performance evaluation index. The change of member bearing capacity is studied through the factors such as the diameter of steel bar, the minimum thickness of concrete cover, and the corrosion rate of steel bar. The impact on the member bearing capacity is considered, and other mechanical properties of the member are analyzed. The relevant influence parameters are input into the BIM model, which is used as the evaluation index of member bearing capacity in the BIM database.

Thirdly, the information of the structure level is added to the information model of the influencing factors of concrete structure stability. The research on the structure level of concrete stability mainly includes two aspects, one is the stability design of the proposed concrete structure, and the other is the stability evaluation and life prediction of the in-service concrete structure. The stability of the structure is evaluated according to the design years, environmental categories, damage parameters, and reliability theory, and these indicators are added to the building information model and integrated into the BIM database according to the level.

2.3 Stability Testing

Build a stability detection network model based on YOLOv4 network architecture, and implement the stability detection of building load-bearing structures. The data in BIM model of building load-bearing structure is used as input data of network model to realize stability detection.

The stability detection network model structure includes three parts: the backbone feature extraction network CSPParknet53, the enhanced feature extraction network (SPP and PANet) and YOLO Head. The input size of the data can select multiple resolutions. After a series of convolution, standardization and activation functions, the input data is continuously downsampled, the scale of the feature layer is continuously reduced, and the number of channels is continuously increased, thus obtaining more semantic information. In the backbone feature extraction network part, the last three feature layers are selected, which are respectively 8, 16, and 32 times compressed from the original data, and are used to detect three different scale features: small, medium, and large.After acquiring the feature layer, the last feature layer is passed into the SPP structure part after three convolutions. SPP uses pooling kernels of different sizes to perform maximum pooling on the input feature layer, and the pooled results are stacked and passed into the PANet structure after three convolutions. PANet includes two processes of up-sampling

and down-sampling. In the up-sampling process, the lower-layer network is double-upsampled and then stacked with the upper-layer feature layer to achieve feature fusion. In the down-sampling process, the upper-layer network is doubled After downsampling, it is stacked with the lower feature layer to achieve feature fusion [9]. After completing PANet, YOLO Head uses the extracted effective features to predict the results. The three feature layers correspond to three YOLO Heads respectively.

The CIoU loss takes into account three geometric parameters, namely, overlapping area, center point distance, and aspect ratio. In the boundary box regression process, it can converge more quickly and have better performance, making the regression process of the target box more stable. CIoU is used as the loss function of the stability detection network model. The calculation formula of CIoU value is as follows:

$$C_{IoU} = A - \left(\frac{C^2\left(D, D^{gt}\right)}{B^2} + \phi\beta \right) \tag{1}$$

In formula (1), A represents the IoU loss value, and the IoU loss is defined as the difference between 1 and IoU. This method can well reflect the degree of coincidence between the predicted frame and the real frame, and has scale invariance, but when the predicted frame is When it does not intersect with the real box, the sliding gradient will not be provided; B represents the diagonal distance of the smallest closure area that can contain both the prediction box and the real box; $C^2\left(D, D^{gt}\right)$ represents the Euclidean distance between D and D^{gt}; D represents the center point of the prediction box; D^{gt} represents the center point of the ground truth box; ϕ represents the scale threshold; β represents the sliding gradient.

The formula for calculating ϕ is as follows:

$$\phi = \frac{\beta}{1 - A + \beta} \tag{2}$$

The calculation formula of β is as follows:

$$\beta = \frac{4}{\pi^2}\left(arv\tan\frac{f}{g} - arv\tan\frac{f'}{g'} \right)^2 \tag{3}$$

In formula (3), f represents the width of the real frame; g represents the height of the real frame; f' represents the width of the predicted frame; g' represents the height of the predicted frame.

The calculation formula of CIoU loss is as follows:

$$L_{C_{IoU}} = 1 - C_{IoU} \tag{4}$$

The method used for parameter optimization is the momentum method, which adds items related to the previous step size on the basis of the original step size of the small batch random gradient decline, which makes the update direction of the parameter not only determined by the current gradient, but also related to the gradient decline direction accumulated previously. This method updates the gradient by using the accumulated historical gradient information. During the accumulation process, the gradient in direction

A is constantly offset and the gradient in direction B is strengthened, which can accelerate the descent of SGD in the correct direction and reduce the vibration. In addition, the momentum method can avoid the problem that the gradient at the saddle point and the local minimum point is 0, and find a better solution.

Label smoothing is mainly used in multi-classification tasks, using "one-hot" to add noise, reducing the weight of the real sample label category when calculating the loss function, and adjusting the upper limit of the prediction target to a lower value, such as 0.9, in the process of calculating the loss, use this value instead of 1, this method can prevent the model from overfitting during the training process and make the network more robust.

In the target detection algorithm, the adjustment of learning rate has a great impact on the network training performance. When the learning rate is large, it can speed up the learning rate and prevent vibration at the local best point, but it is easy to lead to non convergence of the model training and low accuracy of the model; When the learning rate is low, it can help the model to converge and refine, but it is difficult to jump out of the local optimal value and the convergence speed is slow [10]. Select the method of hierarchical descent.

3 Experimental Tests

In order to test the performance of the proposed test method for the stability of building load-bearing structures, the test experiment is carried out. The test process is as follows: first, train the stability detection network model, and then set the accuracy rate and recall rate as the experimental indicators. Finally, the method in this paper is compared with that in reference [3] (method 1) and reference [4] (method 2).

3.1 Model Training

In the test of the design method, the idea of transfer learning is first used to train the stability detection network model. The pre training weights prepared in advance are used for training. The training process includes freezing thawing training. The specific settings of super parameters are as follows:

(1) The first step is to freeze the first 249 layers of the network (backbone feature extraction network) for training, using the YOLOv4 pre-trained weight file, the frozen generation is set to 50, the batch size is 8, and the initial learning rate is 0.001;
(2) After the 50 generations in the second step, the first 249 layers are unfrozen, the batch size is 2, the learning rate is 0.0001, and a total of 100 generations are trained.

In the training process, early stop is set to automatically end the training when the loss value of the verification set does not decrease for 6 generations, and the model is basically convergent at this time. Adam is initially selected as the optimization algorithm in the training process, and the recommended values are used as the parameters. The attenuation rate is 0.999, and the momentum coefficient is 0.9. The programming language used is Python, compiled through VS Code, the network building platform is

the Keras framework of Windows10, and GPU is used for acceleration. The computer configuration is: Intel (R) Core (TM) i5–10500 CPU@3. 10 GHz, 16 GB and 8 GB NVIDIA GeForce RTX 2060 SUPER.

Use Tensorboard to monitor the changes of training set and validation set loss and learning rate in each generation during the training process, and get the loss change image and learning rate drop., the curve tends to be flat. At the 116th round, since the loss of the validation set of multiple trainings no longer decreases, the network is considered to converge. At this time, the loss of the training set is 2.246, the loss of the validation set is 2.728, and the training is over.

3.2 Evaluation Indicators

In order to evaluate the performance of the trained model, accuracy recall (P-R) curve, AP (Average Precision), mAP (Mean Average Precision), F1 score and other indicators are commonly used as evaluation criteria. When drawing P-R curve and calculating mAP value, accuracy and recall are two important indicators. When calculating the accuracy and recall rate, we must first obtain the equivalent of true positives (TP), false positives (FP), true negatives (TN), false negatives (FN), among which TP represents that positive samples are correctly identified as positive samples, TP represents that negative samples are correctly identified as negative samples, FP represents that negative samples are incorrectly identified as positive samples, and FN represents that positive samples are incorrectly identified as negative samples. On this basis, the calculation formulas of accuracy and recall can be obtained:

$$P_{recision} = \frac{TP}{TP + FP} \tag{5}$$

$$R_{ecall} = \frac{TP}{TP + FN} = \frac{TP}{GT} \tag{6}$$

In formula (6), GT refers to the true label; $P_{recision}$ refers to the ratio of correctly identified positive samples to all identified positive samples, also known as “precision”; R_{ecall} refers to the correctly identified positive samples. The ratio of samples to all true labels.

In this process, it is very important for the network to judge the values of TP, FP and FN. For a certain category, the detector first traverses all GT in the data, and then all detection frames of the category are filtered out according to the initial set confidence threshold. The remaining detection frames are arranged according to the confidence level to judge whether the detection frame with the highest confidence level and the CIoU of GT meet the threshold conditions. If it meets the requirements, the detection frame will be marked as TP, and the detection frames of the same GT will be FP later. If it does not meet the requirements of CIoU, it will be directly marked as FP.It is worth noting that mAP is the final evaluation index of the detection model. After all operations are completed, the final detection result is used as the evaluation standard. NMS will only perform this operation when making predictions, and will not perform NMS operations during testing., because a large number of positive and negative samples are needed to learn during training. In this study, the confidence threshold is set to 0.01 when the

detector detects the class, CIoU is set to 0.5, and the confidence threshold is set to 0.6 when performing non-maximum suppression.

After the quantity of TP, FP and FN is obtained, the accuracy and recall rate under different confidence levels can be calculated according to the formula. The change trend of accuracy and recall rate is reverse. A good detector should keep its accuracy at a high level when the recall rate increases.

3.3 Test Results

In the test, method 1 and method 2 are used respectively to compare the three methods.

Table 3. Accuracy test results

Confidence	$P_{recision}$		
	Design method	Method 1	Method 2
0.10	0.942	0.814	0.796
0.15	0.940	0.813	0.794
0.20	0.935	0.805	0.791
0.25	0.932	0.802	0.790
0.30	0.930	0.796	0.781
0.35	0.928	0.794	0.780
0.40	0.925	0.793	0.778

The test results show that the accuracy of the design method is always higher than 0.920 when the confidence level increases from 0.10 to 0.40, while the highest confidence levels of Method 1 and Method 2 are only 0.814 and 0.796, indicating that the accuracy of the design method is higher than that of the other two comparison methods.

Then test the recall rate data of the three methods under different confidence levels, and the test results are shown in Fig. 3.

The recall rate test data show that the recall rate of the three methods shows an increasing trend in the increase of confidence. The recall rate of the design method is much higher than that of method 1 and method 2, indicating that the detection performance achieved by the design is better.

Finally, the stability detection time of the three methods is tested, and the test results are shown in Fig. 4.

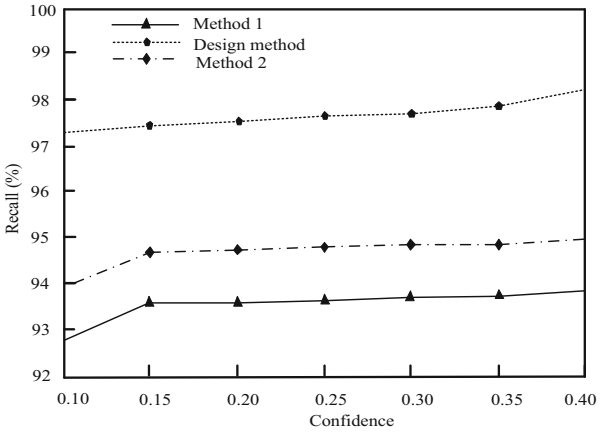

Fig. 3. Recall test data

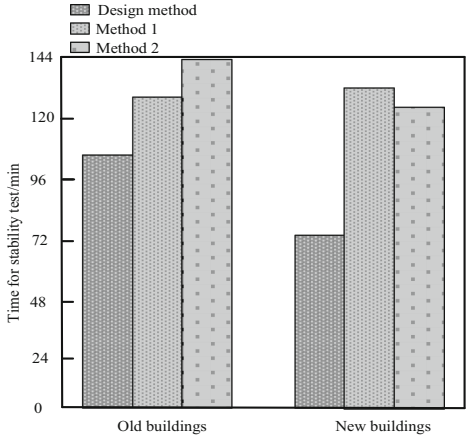

Fig. 4. Stability detection time test results

The above test results show that for new buildings, the stability testing time of the three methods is longer than that of old buildings. Whether it is a new building or an old building, the detection time of the design method is lower than that of the two comparison methods, 106.85 min and 75.41 min respectively.

4 Conclusion

The stability detection of building load-bearing structure is a work involving safety, which must be paid attention to. In the research, a method of building load-bearing structure stability detection based on BIM and computer vision is designed. The image of building load-bearing structure construction is collected by computer vision technology, and the BIM model is built. Finally, the stability detection model is built according to YOLOv4 network architecture, and the stability detection results are obtained.

The experimental results show that the proposed stability detection method can further shorten the detection time based on the detection accuracy. Therefore, it shows that the proposed detection method based on computer vision can effectively improve the reliability of building load-bearing structure stability detection.

References

1. Sgobba, S., Santillana, I.A., Arnau, G., et al.: Examination and assessment of large forged structural components for the precompression structure of the ITER central solenoid[J]. IEEE Trans. Appl. Supercond. Supercond. **30**(9), 1–4 (2020)
2. Guo, W., Yang, W., Ma, Z., et al.: Stability criterion of overburden structure above goaf under buildingload and its application[J]. J. China Coal Soc. **47**(6), 2207–2217 (2022)
3. He, X., Qiu, F., Cheng, X. et al.: High-resolution image building target detection based on edge feature fusion. Comput. Sci. **48**(9), 140–145 (2021)
4. Zhao, R., Wang, J., Lin, S.: Small building detection algorithm based on convolutional neural network. Syst. Eng. Electron. **43**(11), 3098–3106 (2021)
5. Wang, Y., Zhang, Z.: Design of overall stability analysis system for GSCAD building using BIM. Tech. Autom. Appl.Autom. Appl. **41**(11), 175–179 (2022)
6. Lan, Q., Zhang, X., Li, Y., et al.: Output feedback disturbance rejection control for building structure systems subject seismic excitations. Measure. Contr. **53**(10), 1616–1624 (2020)
7. Di, W., Zhe, Z.: Simulation of building space dimension deviation identification based on grid multi density. Comput. Simul. **39**(2), 447–451 (2022)
8. Li, Y., Yue, X., Zhao, L., et al.: Effect of north wall internal surface structure on heat storage-release performance and thermal environment of Chinese solar greenhouse. J. Building Phys. **45**(4), 507–527 (2022)
9. Gu, Y., Li, P., Meng, X., et al.: Re-measurement and stability analysis of super-large structure plane control network. Architect. Technol. **53**(7), 847–850 (2022)
10. Martinez, J., Albeaino, G., Gheisari, M., et al.: UAS point cloud accuracy assessment using structure from motion-based photogrammetry and PPK georeferencing technique for building surveying applications. J. Comput. Civ. Eng.Comput. Civ. Eng. **35**(1), 1–15 (2021)